



ELSEVIER

Contents lists available at ScienceDirect

Thin Solid Films

journal homepage: www.elsevier.com/locate/tsf

Nanostructured CuO films deposited on fluorine doped tin oxide conducting glass with a facile technology

Kenny Padrón^a, Emilio J. Juárez-Pérez^b, Fresnel Forcade^a, Rony Snyders^{c,d}, Xavier Noirfalise^c, Camila Laza^a, Juan Jiménez^a, Elena Vigil^{a,e,*}

^a Materials Science and Technology Institute (IMRE-UH), La Habana, Cuba

^b Photovoltaic and Optoelectronic Devices Group, Departament de Física, Universitat Jaume I, Castello, Spain

^c Materia Nova Research Center, Mons, Belgium

^d Chimie des Interactions Plasma-Surfaces, Center of Innovation and Research in Materials and Polymers (CIRMAP), University of Mons (UMONS), Mons, Belgium

^e Physics Faculty, University of La Habana (UH), Cuba

ARTICLE INFO

Keywords:

CuO thin film
Nanofabrication
Microstructure
Optical properties
Photoelectrode

ABSTRACT

A simple and inexpensive technique to synthesize and deposit Cu(II) oxide (CuO) nanostructured layers is reported herein together with electrical and optical properties characterization. The 2-step deposition procedure consists of spin-coating a Cu(II) formate solution on fluorine-doped tin oxide (FTO) conducting glass substrate followed by a heat treatment. Fluorescence spectroscopy and Fourier transform infrared spectroscopy confirmed that the organic ligand precursor is absent in the obtained film. X-ray diffraction (XRD) experiments show that only CuO films are deposited on the FTO substrate ruling out the presence of other Cu_xO oxides. Scanning-electron microscopy reveals their nanostructured morphology; which agrees with crystallite size domain ($L = 21$ nm) estimated from XRD width peak analysis. Absorption coefficient spectra, as well as direct-gap values ($E_g = 1.52$ – 1.55 eV), were obtained using optical transmittance and reflection spectroscopy. Finally, the as prepared CuO films are used as photoelectrodes in a photoelectrochemical cell with an aqueous electrolyte and short-circuit photocurrent under illumination and dark conditions is measured.

1. Introduction

Nanostructured Cu(II) oxide or cupric oxide (CuO) films have prompted studies for applications in different fields including photovoltaic devices, nanofluids, photodetectors, supercapacitors, field effect transistors and sensors ([1, 2] and references there in). CuO nanostructured films can be obtained using different growth or deposition techniques, for example, spin coating from sol-gel [3], molecular beam epitaxy [4], sputtering [5], electrodeposition [6], successive ionic layer adsorption and reaction method [7], dip coating [8], chemical vapor deposition [9], and chemical bath deposition [10]. However, simple and inexpensive technologies are always preferred using readily available commercial precursors. Particularly, developments on CuO nanostructured photoelectrodes could be beneficial for water splitting applications in spite of recent encouraging results [10]. CuO is considered a p type semiconductor because of Cu atoms vacancies [2]. Reported band gap values are between 1.2 and 2.1 eV [1, 2] – suitable for solar energy converting devices. However, optical and electronic properties in nanostructured CuO films are strongly dependent on size

and morphology of crystalline grain, specially, optical band gap determination is not free of certain kind of controversy. Disagreement exists in the literature regarding its band gap nature. Although mostly reported as a direct band gap semiconductor, some authors have reported an indirect band gap [6, 11, 12]. Contradictory reports also exist regarding conduction and valence band positions. This is essential since water redox levels (H^+/H_2 and OH^-/O_2) must have specific energy values within the semiconductor band gap for non-assisted water splitting. Therefore, the gap value must be higher than 1.23 eV, the energy to break the water molecule. Chiang et al. [13] report for pH 14, valence band position at -5.22 eV and conduction band position at -3.54 eV while Koffyberg and Benko [12] report for pH 9.4, valence band position at -5.42 eV and conduction band position at -4.07 eV. Finally, Nakaoka et al. [14] report for pH 6.8, valence band position at -5.22 eV and conduction band position at -3.66 eV. These values have been translated for pH 14 by Chiang et al [13]. Then, Koffyberg and Benko's values for pH 14 would have been -5.15 eV and -3.80 eV for the valence band and conduction band, respectively. Nakaoka's values would have been -4.80 eV and -3.24 eV, respectively. Finally,

* Corresponding author.

E-mail addresses: ej.juarezperez@oist.jp (E.J. Juárez-Pérez), ffz@imre.uh.cu (F. Forcade), rony.snyders@materianova.be (R. Snyders), xavier.Noirfalise@materianova.be (X. Noirfalise), camila@imre.uh.cu (C. Laza), jjimenez@imre.uh.cu (J. Jiménez), evigil@fisica.uh.cu (E. Vigil).

<https://doi.org/10.1016/j.tsf.2018.06.035>

Received 14 July 2017; Received in revised form 3 May 2018; Accepted 16 June 2018
Available online 19 June 2018

0040-6090/ © 2018 Elsevier B.V. All rights reserved.

Chauhan et al [8, 13] reported values favorable for water splitting as -5.34 eV for valence band position and -3.57 eV for conduction band position.

Herein, a simple and inexpensive technique to synthesize CuO nanostructured layers is presented and the obtained films are overwhelmingly characterized. Cu (II) formate solution is spin-coated onto a fluorine-doped tin oxide (FTO) glass substrate and the films are heat-treated afterwards. No report has been found regarding CuO films obtained using this simple technique. Structural, morphological and optical characteristics of these films have been studied including their behavior as photoelectrodes of photoelectrochemical cells (PEC). Optical absorption coefficient spectra and band gap values of the analyzed CuO thin films are also reported.

2. Experimental details

2.1. CuO films fabrication

Spin-coating was used to deposit the aqueous solution of Cu (II) formate salt. Precursor solutions were prepared by dissolving 135 mg Cu(II) formate hydrate, 97% (Sigma Aldrich) in 1 mL of deionized water with a resistivity > 10 M Ω cm (Milli-Q(r), Millipore Corp.). 100 μ L of this solution were spin-coated onto FTO conducting glass (Tec 15 - Pilkington, area 25×25 mm²) at 2000 rpm during 60 s. After deposition, the precursor solution films on FTO substrates were heat treated at 500 °C during 3 h. The hot plate used was placed inside a laboratory fumehood to avoid excessive ambient temperature and moisture changes. The heater temperature control was permanently checked with a surface thermocouple attached to the heating plate (glass substrates were placed in direct contact with the heating plate). In these conditions, Cu(II) organic salt precursor decomposes obtaining CuO thin films on FTO substrates.

2.2. CuO films structural and optical characteristics

Film morphology was analyzed by scanning electron microscopy (SEM). A Hitachi SU8020 instrument was used for surface imaging. The Cu content was evaluated by means of fluorescence measurements performed with an Oxford Instruments X-Supreme. A Shimadzu IRPrestige21 instrument for Fourier Transform Infrared Spectroscopy (FTIR), equipped with a film measuring unit, was employed to determine CuO vibrational mode peaks. The FTO conducting glass was used as blank for CuO films analysis. The crystal structure was characterized through X-ray diffraction (XRD) experiments conducted with an Empyrean Panalytical diffractometer. Cu $K\alpha$ radiation, $\lambda = 1.5406$ Å, was used for all XRD experiments. From the XRD data, the crystallite size, L , was found using Scherrer expression:

$$L = \frac{K \cdot \lambda}{FWHM \cdot \cos \theta} \quad (1)$$

where K is a constant, frequently approximated to 0.90; λ is the wavelength of X-ray radiation; θ is the Bragg angle; and FWHM (full width at half maximum) is the width in radians at half the maximum intensity of the X-ray diffraction peak at 2θ angle.

Light transmission and reflectance experiments were conducted using a UV–vis–NIR double beam spectrophotometer Cary 5G. Spectra were measured in the 350–950 nm range. The FTO conducting glass was used as blank in light transmission experiments. Film thickness and roughness were monitored using a mechanical surface profiler (Dektak 150).

CuO films were evaluated as photoelectrodes inside a two-electrode photoelectrochemical cell (PEC) system (dimensions $2.5 \times 3.3 \times 4.0$ cm³) as described elsewhere [15]. The CuO/FTO film acted as working photoelectrode and a platinum wire as counter-electrode. A 0.1 M NaOH water-methanol solution (1/1, v/v) was used as electrolyte. Short-circuit photocurrent was measured in a lab-developed

Table 1
CuO films thickness and roughness.

Samples	Thickness (nm)	Roughness (nm) ^a
CuO 400F-1	225	60
CuO 400F-2	229	64
CuO 400F-3	197	70
CuO 400F-4	233	67
CuO 400F-5	210	66

^a Roughness measured by profilometry is equal to the arithmetic average of absolute values of thickness deviations with respect to average thickness.

set-up with an Agilent 34410A multimeter. A 100 mW/cm² light intensity on the photoelectrode was established using a calibrated photodiode. The PEC and its electrical contacts were placed inside a Faraday box which allowed light penetration. Measurements were taken automatically using a Labview program which allows: to control the amperemeter, to plot photocurrent values in real time and to save all the data. Short-circuit photocurrent behavior (0 V applied bias) for light-on and off cycles was registered.

3. Results and discussion

As deposited/synthesized films adhere firmly to the FTO substrate. They are brownish in color, uniform and homogeneous to the naked eye. Profilometry thickness measurements averaged 220 nm with an average roughness of 65 nm (see Table 1). The X-ray fluorescence spectrum corresponding to the bare FTO substrate (Fig. 1a) and CuO film on FTO substrate (Fig. 1b) are compared. The latter spectrum indicates clearly the presence of Cu element by $K_{\alpha 1}$ and $K_{\beta 1}$ peak signature. It also shows that film deposited is rather thin according to the registered intensity counts.

Fig. 2 shows a typical top-view SEM image of sample surface. One can observe the nanostructured morphology and nanocrystal size of $\phi = 20$ –60 nm.

Fig. 3 shows an FTIR spectrum obtained in the 400–1200 cm⁻¹ wavenumber range. No significant vibration peaks belonging to the organic formate ligand can be observed. This confirms the presence of inorganic copper oxide. Indeed, the peak at 536 cm⁻¹ corresponds to the elastic Cu–O vibrational mode [7, 16, 17]. Other modes corresponding to Cu₂O phase [17, 18] are not observed. Therefore, FTIR analysis indicates a complete transformation of Cu(II) formate to CuO during the 3-h-500 °C heating process.

Fig. 4a shows the XRD pattern of CuO films on FTO substrate in the $20^\circ < 2\theta < 60^\circ$ range (θ is the Bragg reflection angle). For the purpose of peak identification, Fig. 4b and c show the reference patterns corresponding to CuO [19] and SnO₂ [20], respectively. In Fig. 4a one can observe peaks at $2\theta = 35.45^\circ$ and $2\theta = 38.66^\circ$ due to Bragg reflections from tenorite CuO planes ($\bar{1}11$) and (111), respectively. Peaks that could correspond to Cu₂O are not observed. Other lines that appear correspond to SnO₂ phase in the FTO glass used as substrate. Scherrer Expression (1) was applied to peak at $2\theta = 35.45^\circ$ which corresponds to tenorite plane ($\bar{1}11$) to find crystallite size. XRD pattern deconvolution was made using OriginPro 2015 software to determine CuO peak FWHM. The obtained values are FWHM = 0.0075 rad and $L = 21$ nm. The calculated crystallite size domain matches smallest nanocrystal areas which abound in top-view SEM figure (Fig. 2). This indicates abundance of monocrystalline nanocrystals.

Transmittance, $T(\lambda)$, and total reflectivity, $R_T(\lambda)$, spectra are shown in Figs. 5 and 6, respectively. The absorption coefficient spectrum, $\alpha(h\nu)$, was obtained substituting in Eq. (2) and using the average sample thickness, d (see Table 1). According to Guillen [21], for each λ value:

$$\alpha = \frac{1}{d} \ln \left[\frac{2R_T^2}{[(1/T)^2(1 - R_T)^4 + 4R_T^2]^{1/2} - (1/T)(1 - R_T)^2} \right] \quad (2)$$

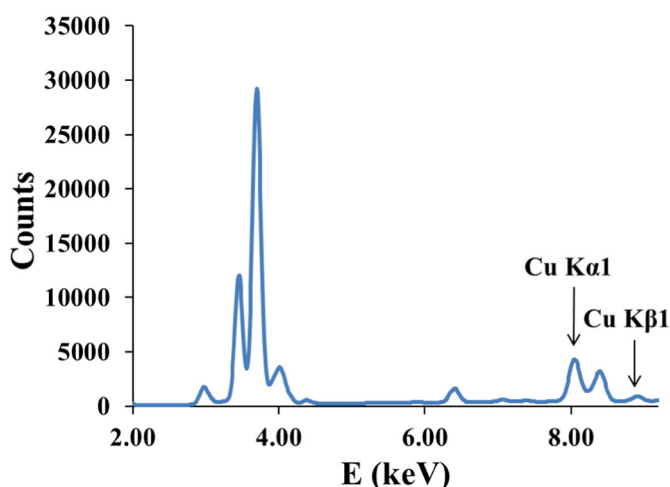
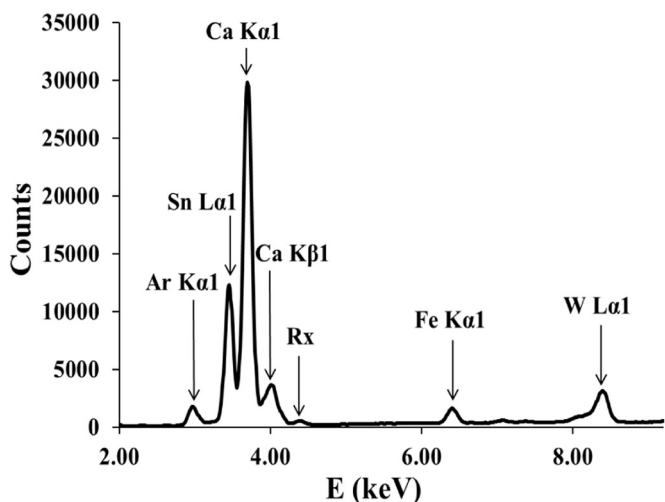


Fig. 1. X-ray fluorescence spectra. (a) FTO conducting glass substrate (b) CuO film on FTO substrate.

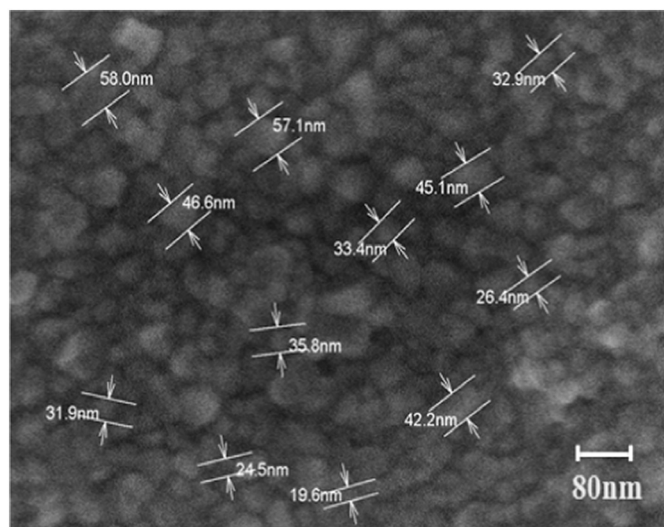


Fig. 2. SEM image of sample surface.

Absorption coefficient spectra are shown in Fig. 7. The logarithmic dependence of $\alpha(h\nu)$ increases abruptly above 1.3 eV indicating the presence of an energy gap (see Fig. 8). Band gap nature and value were determined from Tauc's plots [22] (see Fig. 9). Best-fit to experimental

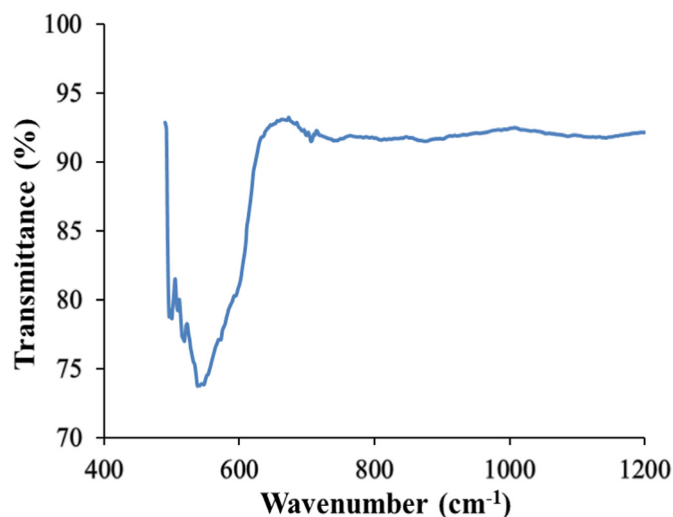


Fig. 3. FTIR spectrum corresponding to the CuO film.

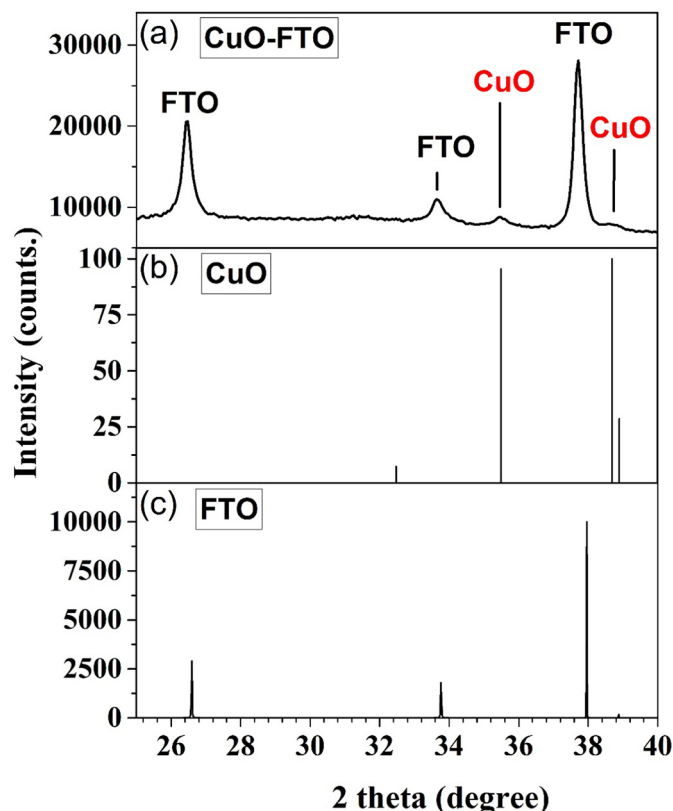


Fig. 4. XRD patterns (a) CuO on FTO experimentally obtained pattern (b) CuO reference pattern [19] (c) FTO reference pattern [20].

data was obtained for $\alpha = \frac{A}{h\nu}(E_g - h\nu)^n$ with $n = 1/2$ for direct gap, in agreement with references [1–3, 5, 7] but not with [6, 10–12, 23]. Additionally, experimental absorption coefficient values in the range of 10^4 cm^{-1} and higher correspond to a direct gap semiconductor. Fig. 9 shows direct gap values $E_g = 1.53 \pm 0.01 \text{ eV}$ and $E_g = 1.54 \pm 0.01 \text{ eV}$ for samples CuO 400F-1 and CuO 400F-2, respectively. These values are higher than the gap value for bulk CuO because of nanocrystalline size morphology confirmed via SEM and XRD measurements on the grown films.

Short-circuit photocurrent behavior is shown in Fig. 10 (CuO films on FTO substrates act as photoelectrodes). The observed photocurrent sense corresponds to a p-type semiconductor: light-created holes go to

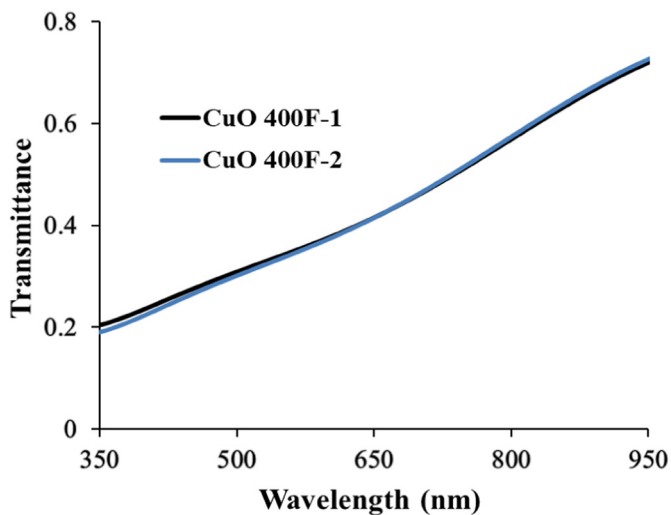


Fig. 5. Typical transmittance spectra of samples CuO 400F-1 and 400F-2.

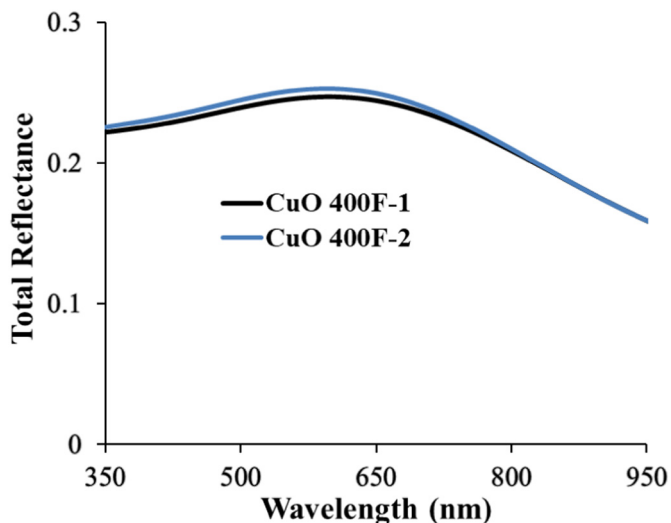


Fig. 6. Typical total reflectance spectra of samples CuO 400F-1 and 400F-2.

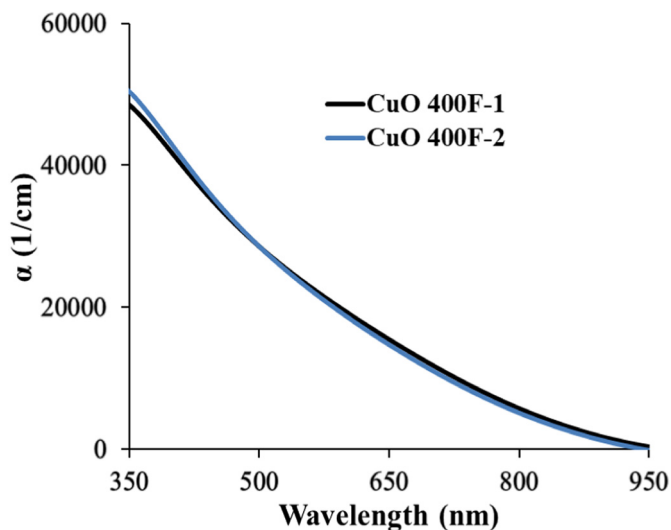


Fig. 7. Absorption coefficient spectra of samples CuO 400F-1 and 400F-2.

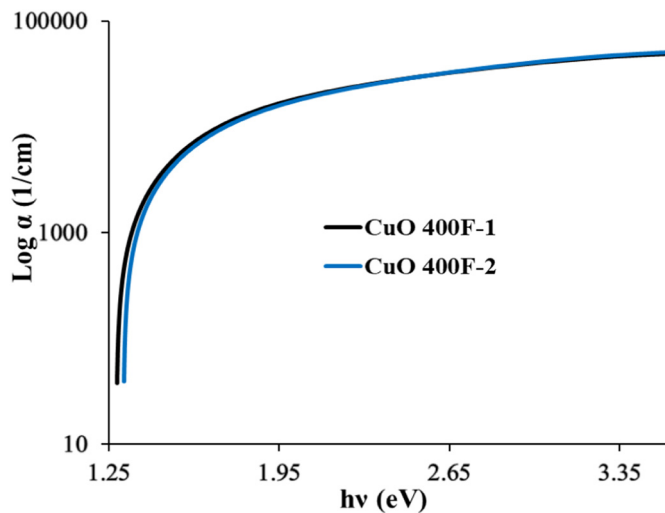


Fig. 8. Absorption coefficient dependence on photon energy for samples CuO 400F-1 and 400F-2 (shown in logarithmic scale).

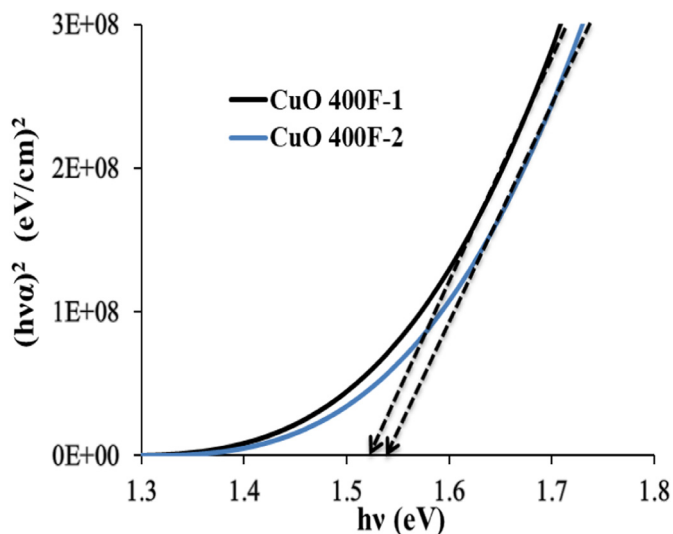


Fig. 9. Tauc's plot for direct energy gap gives $E_g = 1.53 \pm 0.01$ eV and $E_g = 1.54 \pm 0.01$ eV for samples CuO 400F-1 and CuO 400F-2.

the FTO and electrons to the electrolyte. Light response time is < 1 s. Photocurrent spikes are observed whenever light is switched on and photocurrent reaches a stable value in ca. 10 s. This photocurrent transient can be attributed to electrons been trapped in surface states instead of recombining with H^+ ions in the electrolyte [24]. It must be noticed that the spike maximum value is appreciably higher than the stabilization photocurrent (see Fig. 10 and Table 2). Therefore, if surface and/or interfacial traps could be passivated, photocurrent would be considerably larger. On the other hand, photocurrent is not equal to zero for periods of darkness (Fig. 10 and Table 2). This is true for all samples and it is also observed in CuO photocurrent measurements by Dubale A. et al. [25]. This small effect could be due to charge trapped in surface or interfacial states, as well.

4. Conclusions

Well-adhered and homogeneous CuO thin films are grown on conducting FTO substrates using a low-cost and simple spin-coating and thermal heating technique. FTIR and XRD experiments show that Cu(II) oxide is synthesized, i.e., no other Cu oxides nor metallic Cu appear for the applied heat treatment. According to, profilometry, SEM and XRD

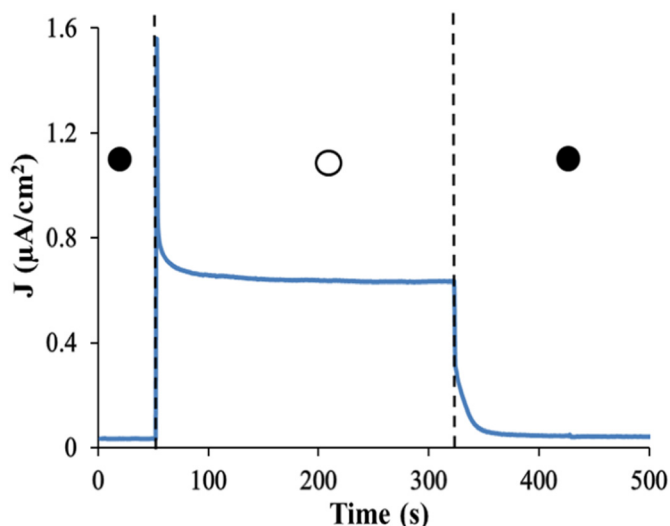


Fig. 10. PEC short-circuit photocurrent density behavior when light is switched on and off.

Table 2

Short-circuit current density measured for several devices using 100 mW/cm² illumination.

Sample	J (μA/cm ²) Dark current	J (μA/cm ²) Light current	
		J _{max} (μA/cm ²) (Maximum peak)	J (μA/cm ²) (Stabilization current)
CuO 400F-2	−0.048	−1.69	−0.39
CuO 400F-3	−0.032	−1.56	−0.64
CuO 400F-5	−0.031	−0.94	−0.25

analysis, the ~200 nm thick films are nanocrystalline in 20–60 nm domain size. Transmittance and total reflection spectra are analyzed, and absorption coefficient spectra calculated. This last spectral dependence and Tauc's method show a direct band gap with $E_g = 1.52\text{--}1.55$ eV. These values are higher than bulk CuO gap value due to CuO nanocrystalline morphology. Short-circuit photocurrent measurements in a two-electrode photoelectrochemical cell confirm CuO p-type conductivity. Photocurrent behavior during light-on and light-off cycles is influenced by the presence of carrier traps, most probably, surface and interfacial defects. Their presence explains the observed photocurrent spikes when light is switched on.

Acknowledgments

The authors acknowledge the support of the WBI (Fédération Wallonie-Bruxelles) for the financial support through the project SUB/2012/86559. University of La Habana group acknowledges the support from the Network “Nanotechnologies for Energy of the Latin American Region” of CyTED and his coordinator, Dr. Juan Bisquert, which allowed research in the Photovoltaic and Optoelectronic Devices Group, Universitat Jaume I (CyTED network 511RT0416).

References

- [1] S.A. Zoofakar, A.R. Rani, J.A. Morfa, P.A. O'Mullane, K. Kalantar-Zadeh, Nanostructured copper oxide semiconductors: a perspective on materials, synthesis methods and applications, *J. Mater. Chem. C* 2 (2014) 5247.
- [2] Q. Zhang, K. Zhang, D. Xu, G. Yang, H. Huang, F. Nie, C. Liu, S. Yang, CuO nanostructures: synthesis characterization, growth mechanisms, fundamental properties, and applications, *Prog. Mater. Sci.* 60 (2014) 208–337.
- [3] V. Patil, D. Jundale, S. Pawar, M. Chougule, P. Godse, S. Patil, B. Raut, S. Sen, Nanocrystalline CuO thin films for H₂S monitoring: microstructural and optoelectronic characterization, *J. Sensor Technol.* 1 (2011) 36–46.
- [4] K. Kawaguchi, R. Kita, M. Nishiyama, T. Morishita, Molecular beam epitaxy growth of CuO and Cu₂O films with controlling the oxygen content by the flux ratio of Cu/O⁺, *J. Cryst. Growth* 143 (1994) 221–226.
- [5] M.J. Hong, Y.C. Lin, L.C. Chao, P.H. Lin, B.R. Huang, Cupric and cuprous oxide by reactive ion beam sputter deposition and the photosensing properties of cupric oxide metal-semiconductor-metal Schottky photodiodes, *Appl. Surf. Sci.* 346 (2015) 18–23.
- [6] M. Izaki, O. Nagai, K. Motomura, J. Sasano, Electrodeposition of 1.4-eV-bandgap p-Copper (II) Oxide film with excellent photoactivity, *J. Electrochem. Soc.* 158 (2011) D578–D584.
- [7] K. Mageshwari, R. Sathyamoorthy, Physical properties of nanocrystalline CuO thin films prepared by the SILAR method, *Mater. Sci. Semicond. Process.* 16 (2013) 337–343.
- [8] D. Chauhan, V.R. Satsangi, S. Dass, R. Shrivastav, Preparation and characterization of nanostructured CuO thin films for photoelectrochemical splitting of water, *Bull. Mater. Sci.* 7 (2006) 709–716.
- [9] T. Maruyama, Copper oxide thin films prepared by chemical vapor deposition from copper dipivaloylmethanate, *Sol. Energy Mater. Sol. Cells* 56 (1998) 85–92.
- [10] A. Kushwaha, R.S. Moakhar, G.K.L. Goh, G.K. Dalapati, Morphologically tailored CuO photocathode using aqueous solution technique for enhanced visible light driven water splitting, *J. Photochem. Photobiol. A Chem.* 337 (2017) 54–61.
- [11] V. Dhanasekaran, T. Mahalingam, R. Chandramohan, J.K. Rhee, J.P. Chu, Electrochemical deposition and characterization of cupric oxide thin films, *Thin Solid Films* 520 (2012) 6608–6613.
- [12] F.P. Koffyberg, F.A. Benko, A photoelectrochemical determination of the position of the conduction and valence band edges of p-type CuO, *J. Appl. Phys.* 53 (1982) 1173.
- [13] Y.C. Chian, H.M. Chang, S.H. Liu, Y.C. Tai, S. Ehrman, Process intensification in the production of photocatalyst for solar hydrogen generation, *Ind. Eng. Chem. Res.* 51 (2012) 5207–5215.
- [14] K. Nakaoka, J. Ueyama, K. Ogura, Photoelectrochemical behavior of electro-deposited CuO and Cu₂O thin films on conducting substrates, *J. Electrochem. Soc.* 151 (2004) C661.
- [15] I. Zumeta, R. Espinosa, J.A. Ayllón, X. Doménech, R. Rodríguez-Clemente, E. Vigil, Comparative study of nanocrystalline TiO₂ photoelectrodes based on characteristics of nanopowder used, *Sol. Energy Mater. Sol. Cells* 76 (2003) 15–24.
- [16] R. Khan, M. Vaseem, L.W. Jang, H.J. Yun, B.Y. Hahn, H.I. Lee, Low temperature preparation of CuO nanospheres and urchin-shaped structures via hydrothermal route, *J. Alloys Compd.* 614 (2014) 211–214.
- [17] S.A. Ethiraj, J.D. Kang, Synthesis and characterization of CuO nanowires by a simple wet chemical method, *Nanoscale Res. Lett.* 7 (2012) 1–5.
- [18] U.S. Liyanaarachchi, C.A.N. Fernando, K.L. Foo, U. Hashim, M. Maza, Structural and photoelectrochemical properties of p-Cu₂O nano-surfaces prepared by oxidizing copper sheets with a slow heating rate exhibiting the highest photocurrent and H₂ evaluation rate, *Chin. J. Phys.* 53 (2015) 040803.
- [19] R.T. Downs, M. Wallace, The American mineralogist crystal structure database, *Am. Mineral.* 88 (2003) 247–250.
- [20] Z. Zhou, S. Yuan, J. Fan, Z. Hou, W. Zhou, Z. Du, S. Wu, CuInS₂ quantum dot-sensitized TiO₂ nanorod array photoelectrodes: synthesis and performance optimization, *Nanoscale Res. Lett.* 7 (2012) 652–659.
- [21] C. Guillén, J. Herrero, Optical properties of electrochemically deposited CuInSe₂ thin films, *Sol. Energy Mater.* 23 (1991) 31–45.
- [22] J. Tauc, F. Abeles (Ed.), *Optical Properties of Solids*, 1972 (North-Holland).
- [23] S. Masudy-Panah, K. Radhakrishnan, A. Kumar, I.T. Wong, R. Yi, K.G. Dalapati, Optical bandgap widening and phase transformation of nitrogen doped cupric oxide, *J. Appl. Phys.* 118 (2015) 225301.
- [24] L.M. Peter, Energetics and kinetics of light-driven oxygen evolution at semiconductor electrodes: the example of hematite, *J. Solid State Electrochem.* (2013) 315–326.
- [25] A.A. Dubale, J.C. Pan, G.A. Tamira, M.H. Chen, N.W. Su, H.C. Chen, J. Rick, W.D. Ayele, A.B. Aragaw, F.J. Lee, W.Y. Yang, J.B. Hwang, Heterostructured Cu₂O/CuO decorated with nickel as a highly efficient photocathode for photoelectrochemical water reduction, *J. Mater. Chem. A* 3 (2015) 12482–12499.